URSI GASS 2020, Rome, Italy, 29 August - 5 September 2020

A High-Frequency Solution for the Plane Wave Diffraction from a 90° Metallic Wedge with a Metamaterial Layer on the Top Surface

G. Gennarelli[(1)], and G. Riccio* [(2)]
(1) I.R.E.A. – C.N.R., Naples, Italy
(2) D.I.E.M. – University of Salerno, Fisciano (SA), Italy

Abstract

A uniform asymptotic solution is presented for evaluating the diffraction from a right-angled metallic wedge partially covered by a double negative metamaterial layer. A plane wave is assumed to impact the structure at skew incidence with respect to the edge. The problem is solved by means of an approach that is based on the physical optics approximation of surface currents radiating in the surrounding free space. The analytical procedure provides in a closed form expression of the diffraction matrix in the framework of the uniform geometrical theory of diffraction. The related diffracted field is able to counterbalance the discontinuities of the geometrical optics field, thus producing a continuous total field also in correspondence of the shadow boundaries.

1 Introduction

As well known, the diffraction by an edge in a perfectly conducting (PEC) wedge was studied by Kouyoumjian and Pathak by means of the Uniform Geometrical Theory of Diffraction (UTD) [1]. This last provides a physical comprehension of the scattering mechanisms due to the interaction of the electromagnetic waves with the structure, and is more attractive and efficient than numerical techniques when solving high-frequency problems. Unfortunately, UTD solutions are available only for a limited number of canonical geometries (f.i., UTD does not provide solutions to the diffraction problems involving dielectric wedges).

A Uniform Asymptotic Physical Optics (UAPO) approach has been proposed in recent years to solve two-dimensional canonical diffraction problems concerning penetrable and impenetrable wedges [2]-[10]. Such an analytical procedure employs electric and magnetic PO equivalent surface currents as radiating sources into the considered observation domain, and furnishes closed form expressions for the diffracted field in the UTD framework. Comparisons with data resulting from the use of commercial and "in house" numerical tools have proved the effectiveness of the UAPO solutions. Accordingly, these last are very interesting from the engineering point of view.

This paper tackles the diffraction problem associated to a plane wave impinging at oblique incidence with respect to the edge in a 90° PEC wedge whose horizontal surface is coated by a lossy double negative metamaterial (DNG MTM) layer (see Fig. 1). As well known, negative real parts of permittivity and permeability characterize the DNG MTMs. Such artificial engineered materials have interesting electromagnetic performance at microwave and optical frequencies. The UAPO approach is here employed to supply a reliable solution to the considered problem. Electric and magnetic PO equivalent surface currents are located on the upper surface of the DNG MTM sheet and radiate in the surrounding free space. Obviously, only the electric PO surface current is simply assumed on the PEC surface.

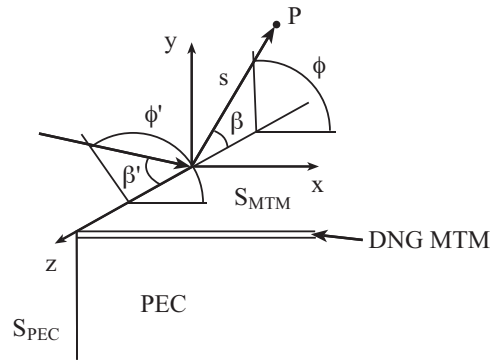

Figure 1. Plane wave diffraction from the considered wedge.

2 The UAPO Diffraction Matrix

The horizontal surface of a 90° PEC wedge is coated by a thin, lossy, isotropic and homogeneous DNG MTM layer with thickness *d* (see Fig. 1). The layer is characterized by the relative electric permittivity $\varepsilon_r = -\varepsilon' - j\varepsilon''$ and the relative magnetic permeability $\mu_r = -\mu' - j\mu''$. Propagation constant and impedance of the surrounding free space are denoted with k_0 and ζ_0, respectively.

If $\underline{k}^i = k_0(-\sin\beta'\cos\phi'\,\hat{x} - \sin\beta'\sin\phi'\,\hat{y} + \cos\beta'\,\hat{z})$ is the propagation vector of the incident plane wave, the electric and magnetic PO equivalent surface currents on the upper surface of the DNG MTM sheet ($y = 0$) can be so expressed:

$$\zeta_0 \underline{J}_s^{MTM} = \left[\left(1-\Gamma_\perp\right) E_\perp^i \sin\beta' \sin\phi' \, \hat{u}_\perp + \left(1+\Gamma_\parallel\right) E_\parallel^i \, \hat{t} \right] \cdot \exp\left(jk_0 \left(x' \sin\beta' \cos\phi' - z' \cos\beta' \right) \right) U_{MTM} \tag{1}$$

$$\underline{J}_{ms}^{MTM} = \left[\left(1-\Gamma_\parallel\right) E_\parallel^i \sin\beta' \sin\phi' \hat{u}_\perp - \left(1+\Gamma_\perp\right) E_\perp^i \, \hat{t} \right] \cdot \exp\left(jk_0 \left(x' \sin\beta' \cos\phi' - z' \cos\beta' \right) \right) U_{MTM} \tag{2}$$

where (x',z') are the co-ordinates of the source point, $\hat{u}_\perp$ is the unit vector perpendicular to the ordinary plane of incidence, $\hat{t} = \hat{y} \times \hat{u}_\perp$, $E_\parallel^i$ and $E_\perp^i$ are the incident electric field components and U_{MTM} is equal to 1 or 0 accounting for the illumination of the DNG MTM surface by $\underline{E}^i$. The reflection coefficients (Γ) for the parallel ($\parallel$) and perpendicular ($\perp$) polarizations are evaluated by means of the Equivalent Transmission Line (ETL) circuit, i.,e.:

$$\Gamma_{\parallel,\perp} = \frac{Z_{\parallel,\perp}^{in} - Z_{\parallel,\perp}^0}{Z_{\parallel,\perp}^{in} + Z_{\parallel,\perp}^0} \tag{3}$$

wherein Z^0 is the ETL characteristic impedance of the surrounding free space and Z^{in} is the ETL input impedance of the DNG MTM layer on the PEC structure [11].

The PO surface current $\underline{J}_s^{PEC} = (-2\hat{x} \times \underline{H}^i) U_{PEC}$ on the uncovered PEC wedge, $\underline{J}_s^{MTM}$ and $\underline{J}_{ms}^{MTM}$ originate the scattered electric field $\underline{E}^s$:

$$\begin{aligned} \underline{E}^s \cong & -jk_0 \iint_{S_{MTM}} \left(\underline{\underline{I}} - \hat{R}\hat{R} \right) \zeta_0 \underline{J}_s^{MTM} \frac{\exp\left(-jk_0 \left| \underline{r} - \underline{r}' \right|\right)}{4\pi \left| \underline{r} - \underline{r}' \right|} dS + \\ & -jk_0 \iint_{S_{MTM}} \left(\underline{J}_{ms}^{MTM} \times \hat{R} \right) \frac{\exp\left(-jk_0 \left| \underline{r} - \underline{r}' \right|\right)}{4\pi \left| \underline{r} - \underline{r}' \right|} dS + \\ & -jk_0 \iint_{S_{PEC}} \left(\underline{\underline{I}} - \hat{R}\hat{R} \right) \zeta_0 \underline{J}_s^{PEC} \frac{\exp\left(-jk_0 \left| \underline{r} - \underline{r}' \right|\right)}{4\pi \left| \underline{r} - \underline{r}' \right|} dS \end{aligned} \tag{4}$$

where $\underline{r}$ and $\underline{r}'$ denote the position vectors of the observation point P and the source point, respectively, $\hat{R} = (\underline{r} - \underline{r}') / \left| \underline{r} - \underline{r}' \right|$ and $\underline{\underline{I}}$ is the 3x3 identity matrix.

According to [2]-[11], the UAPO approach allows one to isolate the high-frequency diffraction contribution that is enclosed in (4). This is possible by using useful analytic approximations and integral evaluations. The result is a closed form expression for the computation of the diffracted field $\underline{E}^d$ in the UTD framework:

$$\begin{pmatrix} E_\beta^d \\ E_\phi^d \end{pmatrix} = \underline{\underline{D}} \frac{\exp(-jk_0 s)}{\sqrt{s}} \begin{pmatrix} E_{\beta'}^i \\ E_{\phi'}^i \end{pmatrix} \tag{5}$$

s representing the distance from the diffraction point to P. The UAPO formulation of the diffraction matrix $\underline{\underline{D}}$ accounts for the individual diffraction contributions related to the horizontal DNG MTM cover and the vertical uncovered PEC surface, i.e.,

$$\underline{\underline{D}} = U_{MTM} I_{MTM}^d \underline{\underline{M}} + U_{PEC} I_{PEC}^d \underline{\underline{N}} . \tag{6}$$

The diffraction functions I_{MTM}^d and I_{PEC}^d include the UTD transition function F_t, but they do not contain information of the involved materials:

$$I_{MTM}^d = \frac{\exp(-j\pi/4)}{2\sqrt{2\pi k_0}} \frac{F_t\left(2k_0 s \sin^2\beta' \cos^2\left(\frac{\phi \pm \phi'}{2} \right) \right)}{\sin^2\beta' (\cos\phi + \cos\phi')} \tag{7}$$

$$I_{PEC}^d = \frac{\exp(-j\pi/4)}{2\sqrt{2\pi k_0}} \cdot \frac{F_t\left(2k_0 s \sin^2\beta' \cos^2\left(\frac{(3\pi/2 - \phi) \pm (3\pi/2 - \phi')}{2} \right) \right)}{\sin^2\beta' \left[\cos(3\pi/2 - \phi) + \cos(3\pi/2 - \phi') \right]} . \tag{8}$$

The choice of the sign + (–) in (7) and (8) depends on the position of P with respect to the wedge surfaces.

The matrices $\underline{\underline{M}}$ and $\underline{\underline{N}}$ account for the expressions of the PO surface currents and are given by:

$$\underline{\underline{M}} = \underline{\underline{M}}_1 \left[\underline{\underline{M}}_2 \underline{\underline{M}}_4 \underline{\underline{M}}_5 + \underline{\underline{M}}_3 \underline{\underline{M}}_4 \underline{\underline{M}}_6 \right] \underline{\underline{M}}_7 \tag{9}$$

$$\underline{\underline{N}} = \underline{\underline{N}}_1 \underline{\underline{N}}_2 \underline{\underline{N}}_3 \underline{\underline{N}}_4 \underline{\underline{N}}_5 \tag{10}$$

with

$$\underline{\underline{M}}_1 = \begin{pmatrix} \cos\beta' \cos\phi & \cos\beta' \sin\phi & -\sin\beta' \\ -\sin\phi & \cos\phi & 0 \end{pmatrix} \tag{11}$$

$$\underline{\underline{M}}_2 = \begin{pmatrix} 1-\sin^2\beta'\cos^2\phi & C(\beta',\phi) \\ B(\beta',\phi) & D(\beta',\phi) \\ C(\beta',\phi) & \sin^2\beta' \end{pmatrix} \quad (12)$$

$$\underline{\underline{M}}_3 = \begin{pmatrix} 0 & -\sin\beta'\sin\phi \\ -\cos\beta' & \sin\beta'\cos\phi \\ \sin\beta'\sin\phi & 0 \end{pmatrix} \quad (13)$$

$$\underline{\underline{M}}_4 = \frac{1}{A(\beta',\phi')} \begin{pmatrix} -\cos\beta' & -\sin\beta'\cos\phi' \\ -\sin\beta'\cos\phi' & \cos\beta' \end{pmatrix} \quad (14)$$

$$\underline{\underline{M}}_5 = \begin{pmatrix} 0 & (1-\Gamma_\perp)\sin\beta'\sin\phi' \\ 1+\Gamma_{\parallel} & 0 \end{pmatrix} \quad (15)$$

$$\underline{\underline{M}}_6 = \begin{pmatrix} (1-\Gamma_{\parallel})\sin\beta'\sin\phi' & 0 \\ 0 & -1-\Gamma_\perp \end{pmatrix} \quad (16)$$

$$\underline{\underline{M}}_7 = \frac{1}{A(\beta',\phi')} \begin{pmatrix} \cos\beta'\sin\phi' & \cos\phi' \\ -\cos\phi' & \cos\beta'\sin\phi' \end{pmatrix} \quad (17)$$

$$\underline{\underline{N}}_1 = \underline{\underline{M}}_1 \quad (18)$$

$$\underline{\underline{N}}_2 = \begin{pmatrix} 1-\sin^2\beta'\cos^2\phi & B(\beta',\phi) & C(\beta',\phi) \\ B(\beta',\phi) & 1-\sin^2\beta'\sin^2\phi & D(\beta',\phi) \\ C(\beta',\phi) & D(\beta',\phi) & \sin^2\beta' \end{pmatrix} \quad (19)$$

$$\underline{\underline{N}}_3 = \frac{1}{A(\beta',\phi')} \begin{pmatrix} 0 & 0 \\ -\cos\beta' & -\sin\beta'\sin\phi' \\ -\sin\beta'\sin\phi' & \cos\beta' \end{pmatrix} \quad (20)$$

$$\underline{\underline{N}}_4 = \begin{pmatrix} 0 & -2\sin\beta'\cos\phi' \\ 2 & 0 \end{pmatrix} \quad (21)$$

$$\underline{\underline{N}}_5 = \frac{1}{A(\beta',\phi')} \begin{pmatrix} -\cos\beta'\sin\phi' & \sin\phi' \\ -\sin\phi' & -\cos\beta'\sin\phi' \end{pmatrix} \quad (22)$$

wherein

$$A(\beta',\phi') = \sqrt{1-\sin^2\beta'\sin^2\phi'} \quad (23)$$

$$B(\beta',\phi) = -\sin^2\beta'\sin\phi\cos\phi \quad (24)$$

$$C(\beta',\phi) = -\sin\beta'\cos\beta'\cos\phi \quad (25)$$

$$D(\beta',\phi) = -\sin\beta'\cos\beta'\sin\phi \quad (26)$$

3 Numerical Examples

The proposed UAPO solution is here tested with respect to its ability to compensate the GO field discontinuities at the reflection boundaries.

The considered DNG MTM layer is characterized by $\varepsilon_r = -3 - j0.01$, $\mu_r = -1 - j0.02$ and $d = 0.2\lambda_0$, where λ_0 is the free-space wavelength. The wedge is lit by an incident plane wave with $E^i_{\beta'} = 1$ and $E^i_{\phi'} = 0$. The incidence direction is $(\beta' = 50°, \phi' = 130°)$. Accordingly, $U_{MTM} = U_{PEC} = 1$ and the reflection boundaries due to the DNG MTM and PEC surfaces occur at $\phi = 50°$ and $\phi = 230°$, respectively. Moreover, the observation domain is a circular path with radius equal to $5\lambda_0$ and $0 < \phi < 270°$.

The jumps of the GO field at the reflection boundaries are evident in Fig. 2 when considering the amplitude of the β-component. As expected, the curve of the UAPO diffracted field possesses two peaks in correspondence of such directions, and its contribution allows one to obtain an unbroken total field as shown in Fig. 3. The ability of the UAPO diffracted field to compensate the discontinuities of the GO field is also confirmed by the results concerning the ϕ-component of the field contributions. GO and UAPO diffracted fields are reported in Fig. 4, whereas the behavior of the total field is depicted in Fig. 5.

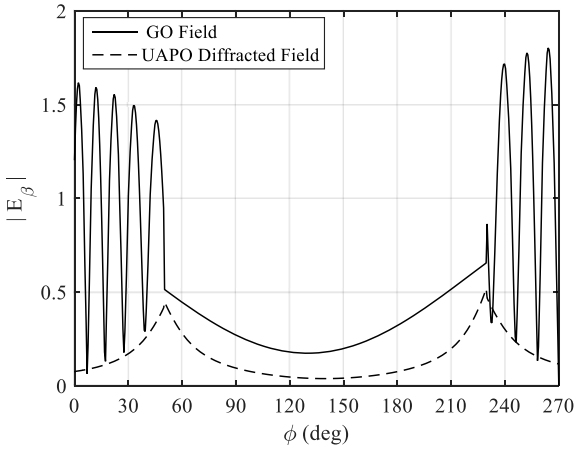

Figure 2. GO field and UAPO diffracted field. Amplitude of the β-component.

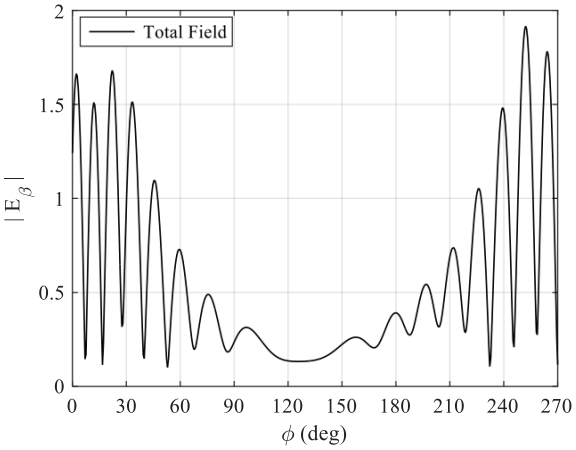

Figure 3. Total field. Amplitude of the β-component.

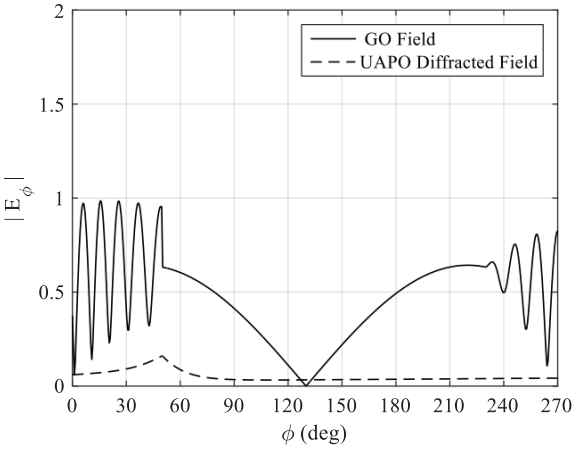

Figure 4. GO field and UAPO diffracted field. Amplitude of the ϕ-component.

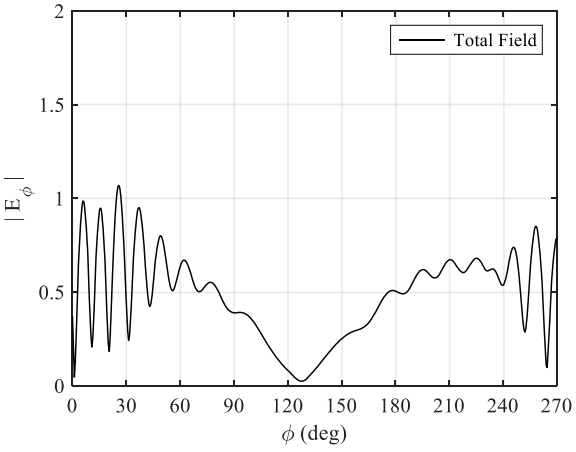

Figure 5. Total field. Amplitude of the ϕ-component.

4 Conclusions and Future Activities

The proposed UAPO solution for the considered diffraction problem in the UTD context has resulted to be user-friendly and able to compensate the GO field jumps. Its accuracy will be tested in a future work by using a full-wave numerical tool.

5 References

1. R. G. Kouyoumjian, and P. H. Pathak, "A uniform geometrical theory of diffraction for an edge in a perfectly conducting surface," *Proc. IEEE,* **62***,* 1974, pp. 1448–1461.

2. C. Gennarelli, G. Pelosi, and G. Riccio, "Approximate diffraction coefficients for an anisotropic impedance wedge," *Electromagnetics,* **21***,* 2001, pp. 165–180.

3. P. Bernardi, R. Cicchetti, C. Gennarelli, G. Pelosi, and G. Riccio, "UAPO solution for the field diffracted by building corners in wireless radio environments," *IEEE Antennas Wireless Propag. Lett.,* **1**, 2002, pp. 169–172.

4. G. Gennarelli, and G. Riccio, "A uniform asymptotic solution for the diffraction by a right-angled dielectric wedge," *IEEE Trans. Antennas Propag.,* **59**, 2011, pp. 898–903.

5. G. Gennarelli, and G. Riccio, "Plane wave diffraction by an obtuse-angled dielectric wedge," *J. Opt. Soc. Am. A,* **28**, 2011, Pages 627–632.

6. G. Gennarelli, and G. Riccio, "Useful solutions for plane wave diffraction by dielectric slabs and wedges," *Int. J. Antennas and Propagation*, **1**, 2012, pp. 1–7.

7. G. Gennarelli, and G. Riccio, "Diffraction by 90° penetrable wedges with finite conductivity," *J. Opt. Soc. Am. A,* **31**, 2014, pp. 21–25.

8. G. Gennarelli, M. Frongillo, and G. Riccio, "High-frequency evaluation of the field inside and outside an acute-angled dielectric wedge," *IEEE Trans. Antennas Propag.*, **63**, 2015, pp. 374–378.

9. M. Frongillo, G. Gennarelli, and G. Riccio, "Plane wave diffraction by arbitrary-angled lossless wedges: high-frequency and time-domain solutions," *IEEE Trans. Antennas Propag*., **66**, 2018, pp. 6646–6653.

10. M. Frongillo, G. Gennarelli, and G. Riccio, "Diffraction by a structure composed of metallic and dielectric 90° blocks, *IEEE Antennas Wireless Propagation Lett.*, **17**, 2018, pp. 881–885.

11. G. Gennarelli, and G. Riccio, "Diffraction by a planar metamaterial junction with PEC backing," *IEEE Trans. Antennas Propag.,* **58**, 2010, pp. 2903–2908.